

Model Coupling for Acoustic Sensors in Layered Media

Ashwin S. Nayak^{1,2}, Andrés Prieto^{1,2}, Daniel Fernández-Comesaña³

14th World Congress on Computational Mechanics

Virtual Congress, 11-15 January 2021

¹Technological Institute of Industrial Mathematics, Spain

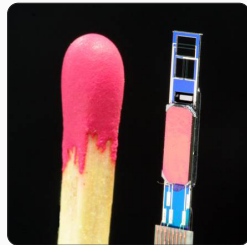
²University of A Coruña, Spain

³Microflown Technologies B.V., Netherlands

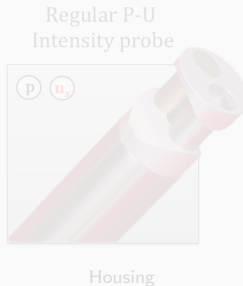


Funded by the EU Horizon 2020 Research and Innovation programme under the Marie Skłodowska-Curie Grant No. 765374.

Problem Statement



Sensor



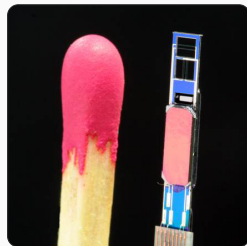
Housing



Windscreen

- The Microflown is a *MEMS* (Micro Electric Mechanical System) which measures particle velocity.
 - Acoustic sensor designed on thermal principle.

Problem Statement



Sensor



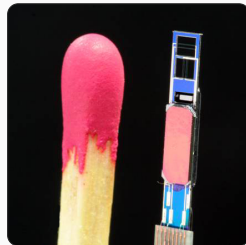
Housing



Windscreen

- Offered in different housings to suit measuring environment.
 - Steel mesh for protection.

Problem Statement



Sensor



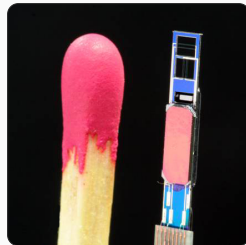
Housing with steel mesh



Windscreen

- Offered in different housings to suit measuring environment.
 - Steel mesh for protection.

Problem Statement



Sensor



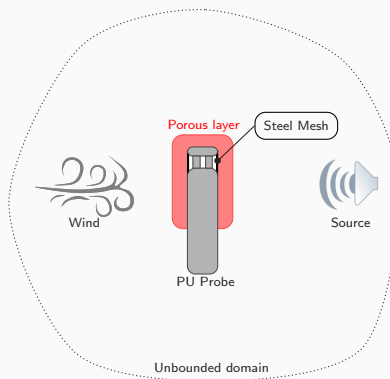
Housing with steel mesh



Windscreen

- Accuracy is *sensitive* to air flow!
 - Porous windscreens suitable upto 15 m/s

Objective

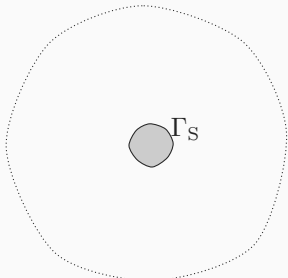


A schematic of the objective coupled problem

Develop *coupled mathematical models* to help design *windscreens* for accurate measurements in windy environments!

Coupled Model : Displacement Formulation

For a given angular frequency $\omega > 0$:



$$-\nabla(\rho_F c_F^2 \operatorname{div} \mathbf{u}_F) - \rho_F \omega^2 \mathbf{u}_F = \mathbf{f}_F \quad \text{in } \Omega_F,$$

$$\mathbf{u}_F \cdot \mathbf{n} = g \quad \text{on } \Gamma_S,$$

$$\rho_F c_F^2 \operatorname{div} u_F^+ - \rho_F c_F^2 \operatorname{div} u_F^- - i\omega Z(\omega) \mathbf{u}_F \cdot \mathbf{n} = 0 \quad \text{on } \Gamma_{MPP},$$

$$u_F^+ \cdot \mathbf{n} - u_F^- \cdot \mathbf{n} = 0 \quad \text{on } \Gamma_{MPP},$$

$$-\nabla(K_P(\omega) \operatorname{div} \mathbf{u}_P) - \rho_P(\omega) \omega^2 \mathbf{u}_P = \mathbf{0} \quad \text{in } \Omega_P,$$

$$\rho_F c_F^2 \operatorname{div} \mathbf{u}_F - K_P(\omega) \operatorname{div} \mathbf{u}_P = \mathbf{0} \quad \text{on } \Gamma_P,$$

$$\mathbf{u}_F \cdot \mathbf{n} - \mathbf{u}_P \cdot \mathbf{n} = 0 \quad \text{on } \Gamma_P,$$

$$\lim_{|x| \rightarrow \infty} |x| \left(\operatorname{div} \mathbf{u}_F - ik_F \mathbf{u}_F \cdot \frac{x}{|x|} \right) = \mathbf{0}, \quad \text{on } \Gamma_\infty,$$

$\square \Omega_F$

Ω_F : Fluid domain, Γ_S : structure boundary

ρ_F : fluid mass density, c_F : sound speed,

\mathbf{f}_F : source field, g : normal displacement,

\mathbf{u}_F : fluid displacement field, \mathbf{n} : surface normal.

Assumptions: Isotropic, Non-viscous, compressible, isentropic **still** acoustic fluid.

Coupled Model : Displacement Formulation

For a given angular frequency $\omega > 0$:

$$\begin{aligned} -\nabla(\rho_F c_F^2 \operatorname{div} u_F) - \rho_F \omega^2 u_F &= f_F \quad \text{in } \Omega_F, \\ u_F \cdot n &= g \quad \text{on } \Gamma_S, \\ \rho_F c_F^2 \operatorname{div} u_F^+ - \rho_F c_F^2 \operatorname{div} u_F^- - i\omega Z(\omega) u_F \cdot n &= 0 \quad \text{on } \Gamma_{MPP}, \\ u_F^+ \cdot n - u_F^- \cdot n &= 0 \quad \text{on } \Gamma_{MPP}, \\ -\nabla(K_P(\omega) \operatorname{div} u_P) - \rho_P(\omega) \omega^2 u_P &= 0 \quad \text{in } \Omega_P, \\ \rho_F c_F^2 \operatorname{div} u_F - K_P(\omega) \operatorname{div} u_P &= 0 \quad \text{on } \Gamma_P, \\ u_F \cdot n - u_P \cdot n &= 0 \quad \text{on } \Gamma_P, \\ \lim_{|x| \rightarrow \infty} |x| \left(\operatorname{div} u_F - ik_F u_F \cdot \frac{x}{|x|} \right) &= 0, \quad \text{on } \Gamma_\infty, \end{aligned}$$

$\square \Omega_F$

Γ_{MPP} : fluid-steel mesh interface, MPP : micro-perforated panel

u_F^+, u_F^- : fluid displacement field along and against the surface normal,

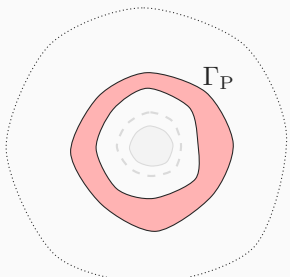
$Z(\omega)$: normal impedance of surface.

Assumptions: *Thin locally reacting panel.*



Coupled Model : Displacement Formulation

For a given angular frequency $\omega > 0$:



Ω_F Ω_P

$$\begin{aligned} -\nabla(\rho_F c_F^2 \operatorname{div} \mathbf{u}_F) - \rho_F \omega^2 \mathbf{u}_F &= \mathbf{f}_F && \text{in } \Omega_F, \\ \mathbf{u}_F \cdot \mathbf{n} &= g && \text{on } \Gamma_S, \\ \rho_F c_F^2 \operatorname{div} \mathbf{u}_F^+ - \rho_F c_F^2 \operatorname{div} \mathbf{u}_F^- - i\omega Z(\omega) \mathbf{u}_F \cdot \mathbf{n} &= 0 && \text{on } \Gamma_{MPP}, \\ \mathbf{u}_F^+ \cdot \mathbf{n} - \mathbf{u}_F^- \cdot \mathbf{n} &= 0 && \text{on } \Gamma_{MPP}, \\ -\nabla(K_P(\omega) \operatorname{div} \mathbf{u}_P) - \rho_P(\omega) \omega^2 \mathbf{u}_P &= \mathbf{0} && \text{in } \Omega_P, \\ \rho_F c_F^2 \operatorname{div} \mathbf{u}_F - K_P(\omega) \operatorname{div} \mathbf{u}_P &= 0 && \text{on } \Gamma_P, \\ \mathbf{u}_F \cdot \mathbf{n} - \mathbf{u}_P \cdot \mathbf{n} &= 0 && \text{on } \Gamma_P, \\ \lim_{|x| \rightarrow \infty} |x| \left(\operatorname{div} \mathbf{u}_F - ik_F \mathbf{u}_F \cdot \frac{x}{|x|} \right) &= 0, && \text{on } \Gamma_\infty, \end{aligned}$$

Ω_P : Porous domain, Γ_P : porous-fluid boundary,

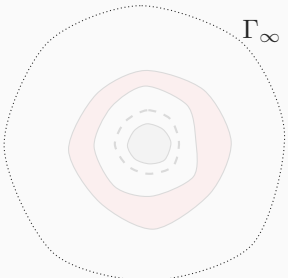
ρ_P : dynamic porous mass density, K_p : dynamic bulk modulus,

\mathbf{u}_P : porous displacement field.

Assumptions: Isotropic, isothermal porous material modeled as equivalent fluid.

Coupled Model : Displacement Formulation

For a given angular frequency $\omega > 0$:



Ω_F Ω_P

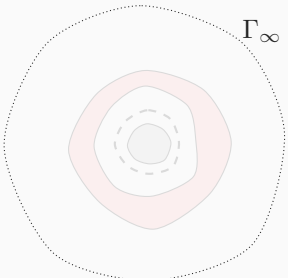
$$\begin{aligned} -\nabla(\rho_F c_F^2 \operatorname{div} \mathbf{u}_F) - \rho_F \omega^2 \mathbf{u}_F &= \mathbf{f}_F && \text{in } \Omega_F, \\ \mathbf{u}_F \cdot \mathbf{n} &= g && \text{on } \Gamma_S, \\ \rho_F c_F^2 \operatorname{div} \mathbf{u}_F^+ - \rho_F c_F^2 \operatorname{div} \mathbf{u}_F^- - i\omega Z(\omega) \mathbf{u}_F \cdot \mathbf{n} &= 0 && \text{on } \Gamma_{MPP}, \\ \mathbf{u}_F^+ \cdot \mathbf{n} - \mathbf{u}_F^- \cdot \mathbf{n} &= 0 && \text{on } \Gamma_{MPP}, \\ -\nabla(K_P(\omega) \operatorname{div} \mathbf{u}_P) - \rho_P(\omega) \omega^2 \mathbf{u}_P &= \mathbf{0} && \text{in } \Omega_P, \\ \rho_F c_F^2 \operatorname{div} \mathbf{u}_F - K_P(\omega) \operatorname{div} \mathbf{u}_P &= 0 && \text{on } \Gamma_P, \\ \mathbf{u}_F \cdot \mathbf{n} - \mathbf{u}_P \cdot \mathbf{n} &= 0 && \text{on } \Gamma_P, \\ \lim_{|\mathbf{x}| \rightarrow \infty} |\mathbf{x}| \left(\operatorname{div} \mathbf{u}_F - ik_F \mathbf{u}_F \cdot \frac{\mathbf{x}}{|\mathbf{x}|} \right) &= \mathbf{0}, && \text{on } \Gamma_\infty, \end{aligned}$$

Γ_∞ : Domain boundary at infinity, $k_F = \omega/c_F$: fluid wavenumber.

Sommerfeld radiation condition : No reflected waves.

Coupled Model : Displacement Formulation

For a given angular frequency $\omega > 0$:



$$\begin{aligned} -\nabla(\rho_F c_F^2 \operatorname{div} \mathbf{u}_F) - \rho_F \omega^2 \mathbf{u}_F &= \mathbf{f}_F && \text{in } \Omega_F, \\ \mathbf{u}_F \cdot \mathbf{n} &= g && \text{on } \Gamma_S, \\ \rho_F c_F^2 \operatorname{div} \mathbf{u}_F^+ - \rho_F c_F^2 \operatorname{div} \mathbf{u}_F^- - i\omega Z(\omega) \mathbf{u}_F \cdot \mathbf{n} &= 0 && \text{on } \Gamma_{MPP}, \\ \mathbf{u}_F^+ \cdot \mathbf{n} - \mathbf{u}_F^- \cdot \mathbf{n} &= 0 && \text{on } \Gamma_{MPP}, \\ -\nabla(K_P(\omega) \operatorname{div} \mathbf{u}_P) - \rho_P(\omega) \omega^2 \mathbf{u}_P &= \mathbf{0} && \text{in } \Omega_P, \\ \rho_F c_F^2 \operatorname{div} \mathbf{u}_F - K_P(\omega) \operatorname{div} \mathbf{u}_P &= 0 && \text{on } \Gamma_P, \\ \mathbf{u}_F \cdot \mathbf{n} - \mathbf{u}_P \cdot \mathbf{n} &= 0 && \text{on } \Gamma_P, \\ \lim_{|\mathbf{x}| \rightarrow \infty} |\mathbf{x}| \left(\operatorname{div} \mathbf{u}_F - ik_F \mathbf{u}_F \cdot \frac{\mathbf{x}}{|\mathbf{x}|} \right) &= \mathbf{0}, && \text{on } \Gamma_\infty, \end{aligned}$$

Ω_F Ω_P

Γ_∞ : Domain boundary at infinity, $k_F = \omega/c_F$: fluid wavenumber.

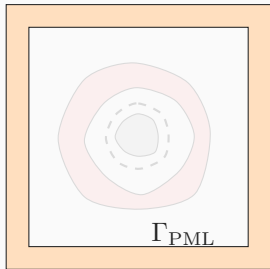
Sommerfeld radiation condition : No reflected waves.

Practically harder to implement. Replaced by a complementary model!

→ Perfectly Matched Layer (PML)

Coupled Model : Displacement Formulation

For a given angular frequency $\omega > 0$:



Ω_F Ω_P Ω_{PML}

$$\begin{aligned}
 -\nabla(\rho_F c_F^2 \operatorname{div} \mathbf{u}_F) - \rho_F \omega^2 \mathbf{u}_F &= \mathbf{f}_F && \text{in } \Omega_F, \\
 \mathbf{u}_F \cdot \mathbf{n} &= g && \text{on } \Gamma_S, \\
 \rho_F c_F^2 \operatorname{div} \mathbf{u}_F^+ - \rho_F c_F^2 \operatorname{div} \mathbf{u}_F^- - i\omega Z(\omega) \mathbf{u}_F \cdot \mathbf{n} &= 0 && \text{on } \Gamma_{\text{MPP}}, \\
 \mathbf{u}_F^+ \cdot \mathbf{n} - \mathbf{u}_F^- \cdot \mathbf{n} &= 0 && \text{on } \Gamma_{\text{MPP}}, \\
 -\nabla(K_P(\omega) \operatorname{div} \mathbf{u}_P) - \rho_P(\omega) \omega^2 \mathbf{u}_P &= \mathbf{0} && \text{in } \Omega_P, \\
 \rho_F c_F^2 \operatorname{div} \mathbf{u}_F - K_P(\omega) \operatorname{div} \mathbf{u}_P &= 0 && \text{on } \Gamma_P, \\
 \mathbf{u}_F \cdot \mathbf{n} - \mathbf{u}_P \cdot \mathbf{n} &= 0 && \text{on } \Gamma_P, \\
 -\operatorname{div}(\rho_F c_F^2 \tilde{\mathbf{C}}(\nabla \mathbf{u}_{\text{PML}})) - \rho_F \omega^2 \tilde{\mathbf{M}} \mathbf{u}_{\text{PML}} &= \mathbf{0} && \text{in } \Omega_{\text{PML}}, \\
 \mathbf{u}_F \cdot \mathbf{n} - \mathbf{u}_{\text{PML}} \cdot \mathbf{n} &= 0 && \text{on } \Gamma_{\text{PML}}, \\
 \rho_F c_F^2 \operatorname{div} \mathbf{u}_F - \rho_F c_F^2 \operatorname{div} \mathbf{u}_{\text{PML}} &= 0 && \text{on } \Gamma_{\text{PML}}.
 \end{aligned}$$

Ω_{PML} : Perfectly-matched layer (PML), Γ_{PML} : Fluid-PML interface,

$\tilde{\mathbf{C}}$: 4th order stretch tensor, $\tilde{\mathbf{M}}$: stretch factor matrix,

\mathbf{u}_{PML} : PML displacement field.

The PML acts as a '*sponge layer*' which absorbs outgoing waves.

Coupled Model : Displacement Formulation

For a given angular frequency $\omega > 0$:



$\square \Omega_F$ $\square \Omega_P$ $\square \Omega_{PML}$

$$\begin{aligned}
 -\nabla(\rho_F c_F^2 \operatorname{div} \mathbf{u}_F) - \rho_F \omega^2 \mathbf{u}_F &= \mathbf{f}_F && \text{in } \Omega_F, \\
 \mathbf{u}_F \cdot \mathbf{n} &= g && \text{on } \Gamma_S, \\
 \rho_F c_F^2 \operatorname{div} \mathbf{u}_F^+ - \rho_F c_F^2 \operatorname{div} \mathbf{u}_F^- - i\omega Z(\omega) \mathbf{u}_F \cdot \mathbf{n} &= 0 && \text{on } \Gamma_{MPP}, \\
 \mathbf{u}_F^+ \cdot \mathbf{n} - \mathbf{u}_F^- \cdot \mathbf{n} &= 0 && \text{on } \Gamma_{MPP}, \\
 -\nabla(K_P(\omega) \operatorname{div} \mathbf{u}_P) - \rho_P(\omega) \omega^2 \mathbf{u}_P &= \mathbf{0} && \text{in } \Omega_P, \\
 \rho_F c_F^2 \operatorname{div} \mathbf{u}_F - K_P(\omega) \operatorname{div} \mathbf{u}_P &= 0 && \text{on } \Gamma_P, \\
 \mathbf{u}_F \cdot \mathbf{n} - \mathbf{u}_P \cdot \mathbf{n} &= 0 && \text{on } \Gamma_P, \\
 -\operatorname{div}(\rho_F c_F^2 \tilde{\mathbf{C}}(\nabla \mathbf{u}_{PML})) - \rho_F \omega^2 \tilde{\mathbf{M}} \mathbf{u}_{PML} &= \mathbf{0} && \text{in } \Omega_{PML}, \\
 \mathbf{u}_F \cdot \mathbf{n} - \mathbf{u}_{PML} \cdot \mathbf{n} &= 0 && \text{on } \Gamma_{PML}, \\
 \rho_F c_F^2 \operatorname{div} \mathbf{u}_F - \rho_F c_F^2 \operatorname{div} \mathbf{u}_{PML} &= 0 && \text{on } \Gamma_{PML}.
 \end{aligned}$$

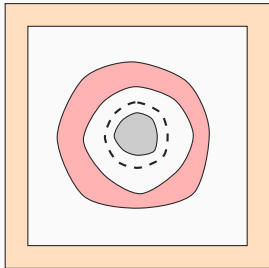
$$\tilde{\mathbf{C}}(\nabla \mathbf{w}) = \left(\sum_{j=1}^3 \frac{1}{\gamma_j} \frac{\partial w_j}{\partial x_j} \right) \mathbf{I}, \quad \text{where, I is the identity matrix.}$$

$$\tilde{\mathbf{M}} = \sum_{j=1}^3 \gamma_j \mathbf{e}_j \otimes \mathbf{e}_j.$$

$\gamma_j \in \mathbb{C}$: Stretch factor in j -th spatial direction.

Coupled Model : Displacement Formulation

For a given angular frequency $\omega > 0$:



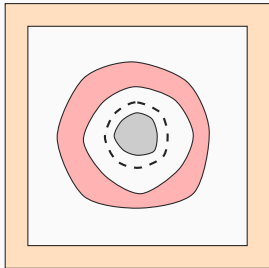
$$\begin{aligned}
 -\nabla(\rho_F c_F^2 \operatorname{div} \mathbf{u}_F) - \rho_F \omega^2 \mathbf{u}_F &= \mathbf{f}_F && \text{in } \Omega_F, \\
 \mathbf{u}_F \cdot \mathbf{n} &= g && \text{on } \Gamma_S, \\
 \rho_F c_F^2 \operatorname{div} \mathbf{u}_F^+ - \rho_F c_F^2 \operatorname{div} \mathbf{u}_F^- - i\omega Z(\omega) \mathbf{u}_F \cdot \mathbf{n} &= 0 && \text{on } \Gamma_{MPP}, \\
 \mathbf{u}_F^+ \cdot \mathbf{n} - \mathbf{u}_F^- \cdot \mathbf{n} &= 0 && \text{on } \Gamma_{MPP}, \\
 -\nabla(K_P(\omega) \operatorname{div} \mathbf{u}_P) - \rho_P(\omega) \omega^2 \mathbf{u}_P &= \mathbf{0} && \text{in } \Omega_P, \\
 \rho_F c_F^2 \operatorname{div} \mathbf{u}_F - K_P(\omega) \operatorname{div} \mathbf{u}_P &= 0 && \text{on } \Gamma_P, \\
 \mathbf{u}_F \cdot \mathbf{n} - \mathbf{u}_P \cdot \mathbf{n} &= 0 && \text{on } \Gamma_P, \\
 -\operatorname{div}(\rho_F c_F^2 \tilde{\mathbf{C}}(\nabla \mathbf{u}_{PML})) - \rho_F \omega^2 \tilde{\mathbf{M}} \mathbf{u}_{PML} &= \mathbf{0} && \text{in } \Omega_{PML}, \\
 \mathbf{u}_F \cdot \mathbf{n} - \mathbf{u}_{PML} \cdot \mathbf{n} &= 0 && \text{on } \Gamma_{PML}, \\
 \rho_F c_F^2 \operatorname{div} \mathbf{u}_F - \rho_F c_F^2 \operatorname{div} \mathbf{u}_{PML} &= 0 && \text{on } \Gamma_{PML}.
 \end{aligned}$$

Ω_F Ω_P Ω_{PML}

Necessary parameters : $Z(\omega)$, $\rho_P(\omega)$, $K_P(\omega)$ and γ_j 's!

Coupled Model : Displacement Formulation

For a given angular frequency $\omega > 0$:



$$\begin{aligned} -\nabla(\rho_F c_F^2 \operatorname{div} \mathbf{u}_F) - \rho_F \omega^2 \mathbf{u}_F &= \mathbf{f}_F && \text{in } \Omega_F, \\ \mathbf{u}_F \cdot \mathbf{n} &= g && \text{on } \Gamma_S, \\ \rho_F c_F^2 \operatorname{div} \mathbf{u}_F^+ - \rho_F c_F^2 \operatorname{div} \mathbf{u}_F^- - i\omega Z(\omega) \mathbf{u}_F \cdot \mathbf{n} &= 0 && \text{on } \Gamma_{MPP}, \\ \mathbf{u}_F^+ \cdot \mathbf{n} - \mathbf{u}_F^- \cdot \mathbf{n} &= 0 && \text{on } \Gamma_{MPP}, \\ -\nabla(K_P(\omega) \operatorname{div} \mathbf{u}_P) - \rho_P(\omega) \omega^2 \mathbf{u}_P &= \mathbf{0} && \text{in } \Omega_P, \\ \rho_F c_F^2 \operatorname{div} \mathbf{u}_F - K_P(\omega) \operatorname{div} \mathbf{u}_P &= 0 && \text{on } \Gamma_P, \\ \mathbf{u}_F \cdot \mathbf{n} - \mathbf{u}_P \cdot \mathbf{n} &= 0 && \text{on } \Gamma_P, \\ -\operatorname{div}(\rho_F c_F^2 \tilde{\mathbf{C}}(\nabla \mathbf{u}_{PML})) - \rho_F \omega^2 \tilde{\mathbf{M}} \mathbf{u}_{PML} &= \mathbf{0} && \text{in } \Omega_{PML}, \\ \mathbf{u}_F \cdot \mathbf{n} - \mathbf{u}_{PML} \cdot \mathbf{n} &= 0 && \text{on } \Gamma_{PML}, \\ \rho_F c_F^2 \operatorname{div} \mathbf{u}_F - \rho_F c_F^2 \operatorname{div} \mathbf{u}_{PML} &= 0 && \text{on } \Gamma_{PML}. \end{aligned}$$

Ω_F Ω_P Ω_{PML}

Necessary parameters : $Z(\omega)$, $\rho_P(\omega)$, $K_P(\omega)$ and γ_j 's!

PML Stretch factors, γ_j 's

For $\Omega_{\text{PML}} = \prod_{j=1}^3 [-L_j^\infty, L_j^\infty] \setminus \prod_{j=1}^3 [-L_j, L_j]$,

$\gamma_j \in \mathbb{C}$, $j = 1, 2, 3$ are modeled by a piecewise smooth function,

$$\gamma_j(x_j) = \begin{cases} 1 & |x_j| \leq L_j, \\ 1 + i\sigma_j(x_j) & L_j \leq |x_j| \leq L_j^\infty, \end{cases}$$

where, σ_j is the absorption function.

Optimal Absorption function¹:

$$\sigma_j(x_j) = \frac{c_F}{\omega |L_j^\infty - x_j|}$$

¹Bermúdez et al., “An optimal perfectly matched layer with unbounded absorbing function for time-harmonic acoustic scattering problems”.

PML Stretch factors, γ_j 's

For $\Omega_{\text{PML}} = \prod_{j=1}^3 [-L_j^\infty, L_j^\infty] \setminus \prod_{j=1}^3 [-L_j, L_j]$,

$\gamma_j \in \mathbb{C}$, $j = 1, 2, 3$ are modeled by a piecewise smooth function,

$$\gamma_j(x_j) = \begin{cases} 1 & |x_j| \leq L_j, \\ 1 + i\sigma_j(x_j) & L_j \leq |x_j| \leq L_j^\infty, \end{cases}$$

where, σ_j is the absorption function.

Optimal Absorption function¹:

$$\sigma_j(x_j) = \frac{c_F}{\omega |L_j^\infty - x_j|}$$

¹Bermúdez et al., “An optimal perfectly matched layer with unbounded absorbing function for time-harmonic acoustic scattering problems”.

Steel Mesh Impedance, $Z(\omega)$

*Locally-reactive panel impedance models*²

- Assumes equivalence to a *thin* perforated panel with circular 'holes'.
- Expression for surface impedance with parameters
 - d : orifice diameter ,
 - p : Ratio of perforated area, and
 - t : thickness of panel.

$$Z(\omega) = \frac{32\eta_F t}{pd^2} \left(\sqrt{1 + \frac{s^2}{32}} + \sqrt{\frac{sd}{4t}} \right) + i \frac{\rho_F \omega t}{p} \left(1 + \frac{1}{\sqrt{9 + s^2/2}} + \frac{0.85d}{t} \right),$$

with,

$$s = d \sqrt{\frac{\rho_F \omega}{4\eta_F}},$$

η_F : Fluid viscosity

²Maa, "Microperforated-Panel Wideband Absorbers".

Steel Mesh Impedance, $Z(\omega)$

Locally-reactive panel impedance models

- Assumes equivalence to a *thin* perforated panel with circular 'holes'.
- Expression for surface impedance with parameters
 - d : orifice diameter ,
 - p : Ratio of perforated area, and
 - t : thickness of panel.

$$Z(\omega) = \frac{32\eta_F t}{pd^2} \left(\sqrt{1 + \frac{s^2}{32}} + \sqrt{\frac{sd}{4t}} \right) + i \frac{\rho_F \omega t}{p} \left(1 + \frac{1}{\sqrt{9 + s^2/2}} + \frac{0.85d}{t} \right),$$

with,

$$s = d \sqrt{\frac{\rho_F \omega}{4\eta_F}},$$

η_F : Fluid viscosity

Steel Mesh Impedance, $Z(\omega)$

Locally-reactive panel impedance models

- Assumes equivalence to a *thin* perforated panel with circular 'holes'.
- Expression for surface impedance with parameters
 - d : orifice diameter ,
 - p : Ratio of perforated area, and
 - t : thickness of panel.

$$Z(\omega) = \frac{32\eta_F t}{pd^2} \left(\sqrt{1 + \frac{s^2}{32}} + \sqrt{\frac{sd}{4t}} \right) + i \frac{\rho_F \omega t}{p} \left(1 + \frac{1}{\sqrt{9 + s^2/2}} + \frac{0.85d}{t} \right),$$

with,

$$s = d \sqrt{\frac{\rho_F \omega}{4\eta_F}},$$

η_F : Fluid viscosity

Parameters easily obtained from manufacturers!

Porous parameters, $\rho_P(\omega)$ and $K_P(\omega)$: JCAL Model

Johnson-Champoux-Allard-Lafarge (JCAL) model²

- Valid for porous materials with arbitrarily shaped pores
- Six-parameter model to describe rigid-frame porous media properties

$$\rho_P(\omega) = \frac{\rho_F}{\phi} \alpha_\infty \left(1 - i \frac{\sigma \phi}{\omega \rho_F \alpha_\infty} \sqrt{1 + i \frac{4\alpha_\infty^2 \eta \rho_F \omega}{\sigma^2 \Lambda^2 \phi^2}} \right),$$

$$K_P(\omega) = \frac{\gamma P_F / \phi}{\gamma - (\gamma - 1) \left(1 - i \frac{\eta \phi}{\rho_F k'_0 \omega \text{Pr}} \sqrt{1 + i \frac{4{k'_0}^2 \rho_F \omega \text{Pr}}{\eta \Lambda'^2 \phi^2}} \right)^{-1}};$$

²Champoux and J.-F. Allard, "Dynamic tortuosity and bulk modulus in air-saturated porous media".

Porous parameters, $\rho_P(\omega)$ and $K_P(\omega)$: JCAL Model

Johnson-Champoux-Allard-Lafarge (JCAL) model

- Valid for porous materials with arbitrarily shaped pores
- Six-parameter model to describe rigid-frame porous media properties

$$\rho_P(\omega) = \frac{\rho_F}{\phi} \alpha_\infty \left(1 - i \frac{\sigma \phi}{\omega \rho_F \alpha_\infty} \sqrt{1 + i \frac{4\alpha_\infty^2 \eta \rho_F \omega}{\sigma^2 \Lambda^2 \phi^2}} \right),$$

$$K_P(\omega) = \frac{\gamma P_F / \phi}{\gamma - (\gamma - 1) \left(1 - i \frac{\eta \phi}{\rho_F k'_0 \omega \text{Pr}} \sqrt{1 + i \frac{4{k'_0}^2 \rho_F \omega \text{Pr}}{\eta \Lambda'^2 \phi^2}} \right)^{-1}};$$

Fluid Parameters:

ρ_F : fluid mass density, γ : specific heat ratio,

Pr : Prandtl Number, P_F : equilibrium fluid pressure.

Porous parameters, $\rho_P(\omega)$ and $K_P(\omega)$: JCAL Model

Johnson-Champoux-Allard-Lafarge (JCAL) model

- Valid for porous materials with arbitrarily shaped pores
- Six-parameter model to describe rigid-frame porous media properties

Parameter	#	Typ. Value
Porosity	ϕ	0.9 – 1.0
Flow Resistivity	σ	$4 \times 10^4 \text{ Nsm}^{-4}$
Tourtuosity	α_∞	1.0 – 3.0
Viscous Characteristic Length	Λ	$56 \times 10^{-6} \text{ m}$
Thermal Characteristic Length	Λ'	$110 \times 10^{-6} \text{ m}$
Static Thermal Permeability	k_0'	2.5×10^{-10}

ϕ, σ : experimentally measurable.

α_∞ : experimentally measurable but only at high frequencies

Λ, Λ', k_0' : not easily measured by experiments

Porous parameters, $\rho_P(\omega)$ and $K_P(\omega)$: JCAL Model

Johnson-Champoux-Allard-Lafarge (JCAL) model

- Valid for porous materials with arbitrarily shaped pores
- Six-parameter model to describe rigid-frame porous media properties

Parameter	#	Typ. Value
Porosity	ϕ	0.9 – 1.0
Flow Resistivity	σ	$4 \times 10^4 \text{ Nsm}^{-4}$
Tourtuosity	α_∞	1.0 – 3.0
Viscous Characteristic Length	Λ	$56 \times 10^{-6} \text{ m}$
Thermal Characteristic Length	Λ'	$110 \times 10^{-6} \text{ m}$
Static Thermal Permeability	k_0'	2.5×10^{-10}

ϕ, σ : experimentally measurable.

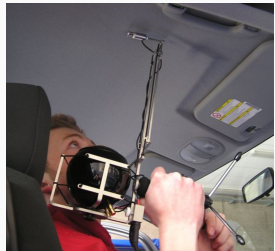
α_∞ : experimentally measurable but only at high frequencies

Λ, Λ', k_0' : not easily measured by experiments

JCAL parameter estimation: inverse problem

Parametric fitting approach through inverse models²:

- Fits surface impedance to experimental values for a porous medium.
- Surface impedance modeled with various porous models including JCAL.
- The Microflown *insitu* impedance setup measures surface impedance, absorption and reflection.



The Microflown *insitu* absorption setup

²Río Martín, “Numerical characterization of complex materials and vibro-acoustic systems”.

JCAL parameter estimation: inverse problem

The JCAL Model parameters are estimated using,

$$\mathbf{p} = \operatorname{argmin}_{\mathbf{p}} \sum_{j=1}^N \frac{\int_{\omega} |Z_{\text{exp}, j}(\omega) - Z(\omega; \mathbf{p})|^2 d(\log \omega)}{\int_{\omega} |Z_{\text{exp}, j}|^2 d(\log \omega)}$$

where,

- $\mathbf{p} = (\phi, \sigma, \alpha_{\infty}, \Lambda, \Lambda', k'_0)^T$,
- $Z_{\text{exp}, j}(\omega)$: Frequency response of measured surface impedance from j -th trial with $j = 1, \dots, N$.
- and, the frequency response of modeled surface impedance for a sample of thickness l (obtained by plane-wave analysis),

$$Z(\omega; \mathbf{p}) = \sqrt{\phi^2 \rho_P(\omega; \mathbf{p}) K_P(\omega; \mathbf{p})} \coth \left(i \frac{\omega^2 \rho_P(\omega; \mathbf{p})}{K_P(\omega; \mathbf{p})} l \right)$$

JCAL parameter estimation: inverse problem

The JCAL Model parameters are estimated using,

$$\mathbf{p} = \operatorname{argmin}_{\mathbf{p}} \sum_{j=1}^N \frac{\int_{\omega} |Z_{\text{exp}, j}(\omega) - Z(\omega; \mathbf{p})|^2 d(\log \omega)}{\int_{\omega} |Z_{\text{exp}, j}|^2 d(\log \omega)}$$

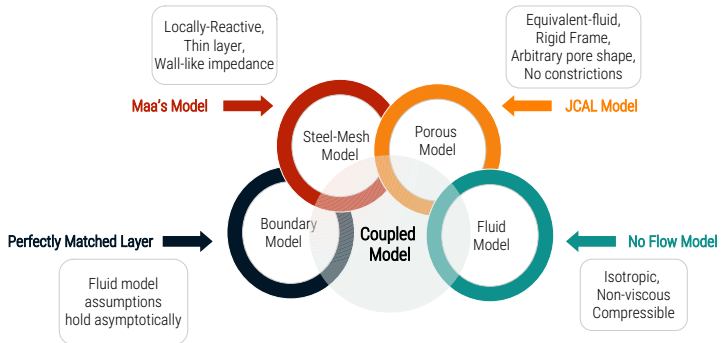
where,

- $\mathbf{p} = (\phi, \sigma, \alpha_{\infty}, \Lambda, \Lambda', k'_0)^T$,
- $Z_{\text{exp}, j}(\omega)$: Frequency response of measured surface impedance from j -th trial with $j = 1, \dots, N$.
- and, the frequency response of modeled surface impedance for a sample of thickness l (obtained by plane-wave analysis),

$$Z(\omega; \mathbf{p}) = \sqrt{\phi^2 \rho_P(\omega; \mathbf{p}) K_P(\omega; \mathbf{p})} \coth \left(i \frac{\omega^2 \rho_P(\omega; \mathbf{p})}{K_P(\omega; \mathbf{p})} l \right)$$

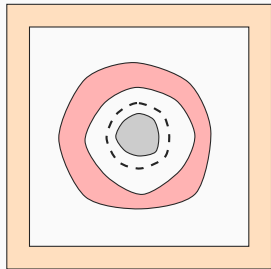
Estimation of all the JCAL parameters is possible!

Model Hierarchy



Hierarchy of all models coupled along with assumptions

Finite Element Method: Variational Form

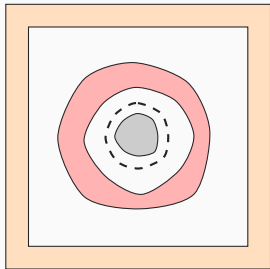


Introduce $\Omega = \Omega_F \cup \Omega_P \cup \Omega_{PML}$ and,

$$\boldsymbol{u} = \begin{cases} \boldsymbol{u}_F & \text{in } \Omega_F, \\ \boldsymbol{u}_P & \text{in } \Omega_P, \\ \boldsymbol{u}_{PML} & \text{in } \Omega_{PML} \end{cases}$$

□ Ω_F ■ Ω_P □ Ω_{PML}

Finite Element Method: Variational Form



Ω_F Ω_P Ω_{PML}

Introduce $\Omega = \Omega_F \cup \Omega_P \cup \Omega_{PML}$ and,

$$u = \begin{cases} u_F & \text{in } \Omega_F, \\ u_P & \text{in } \Omega_P, \\ u_{PML} & \text{in } \Omega_{PML} \end{cases}$$

Remark: Normal displacements have to be continuous across interfaces Γ_{MPP} , Γ_P and Γ_{PML} !

Finite Element Method: Variational Form

Define

$$\mathbf{S} = \left\{ \mathbf{v} \in [\mathbf{L}^2(\Omega)]^3 : \begin{array}{l} \mathbf{v}|_{\Omega_F} \in \mathbf{H}(\text{div}, \Omega_F), \mathbf{v}|_{\Omega_P} \in \mathbf{H}(\text{div}, \Omega_P), \\ \widetilde{\mathbf{M}}\mathbf{v}|_{\Omega_{\text{PML}}} \in [\mathbf{L}^2(\Omega_{\text{PML}})]^3, \\ \widetilde{\text{div}}(\mathbf{v}|_{\Omega_{\text{PML}}}) \in \mathbf{L}^2(\Omega_{\text{PML}}), \mathbf{v} \cdot \mathbf{n} = 0 \text{ on } \Gamma_\infty \end{array} \right\}$$

Variational problem

Given $\omega > 0$, find $\mathbf{u} \in \mathbf{S}$ such that $\mathbf{u} \cdot \mathbf{n} = g$ on Γ_S , and

$$\begin{aligned} & \int_{\Omega_F} \rho_F c_F^2 \operatorname{div} \mathbf{u} \operatorname{div} \mathbf{v} dV - \int_{\Omega_F} \rho_F \omega^2 \mathbf{u} \cdot \mathbf{v} dV \\ & + \int_{\Omega_P} K_P(\omega) \operatorname{div} \mathbf{u} \operatorname{div} \mathbf{v} dV - \int_{\Omega_P} \rho_P(\omega) \omega^2 \mathbf{u} \cdot \mathbf{v} dV \\ & + \int_{\Omega_{\text{PML}}} \rho_F c_F^2 \widetilde{\mathbf{C}}(\nabla \mathbf{u}) : \nabla \mathbf{v} dV - \int_{\Omega_{\text{PML}}} \rho_F \omega^2 \widetilde{\mathbf{M}} \mathbf{u} \cdot \mathbf{v} dV \\ & + \int_{\Gamma_{\text{MPP}}} i\omega Z(\omega) (\mathbf{u} \cdot \mathbf{n})(\mathbf{v} \cdot \mathbf{n}) dS = \int_{\Omega_F} \mathbf{f}_F \cdot \mathbf{v} dV, \end{aligned}$$

for all $\mathbf{v} \in \mathbf{S}$ with $\mathbf{v} \cdot \mathbf{n} = 0$ on Γ_S .

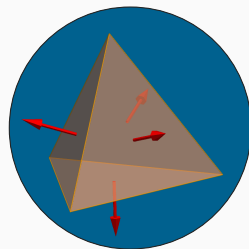
Finite Element Method: Raviart-Thomas

First-order Raviart-Thomas Finite Elements (\mathbf{RT}_h^1) are used for discretization of the functional space \mathbf{S} over a tetrahedral mesh \mathcal{T}_h of Ω .

Raviart-Thomas Finite Element Space

$$\mathbf{RT}_h^1(\Omega) = \left\{ \mathbf{q} \in \mathbf{H}(\text{div}, \Omega) : \mathbf{q}|_T = \mathbf{a}_T + b_T \mathbf{x}, \mathbf{a}_T \in \mathbb{C}^3, b_T \in \mathbb{C}, T \in \mathcal{T}_h \right\}$$

- Basis functions defined on face normals of tetrahedra.
- Constant divergence in each element.
- Completely determined system if their normal components are known on each face.



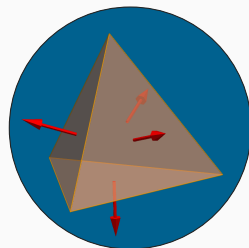
Finite Element Method: Raviart-Thomas

First-order Raviart-Thomas Finite Elements (\mathbf{RT}_h^1) are used for discretization of the functional space \mathbf{S} over a tetrahedral mesh \mathcal{T}_h of Ω .

Raviart-Thomas Finite Element Space

$$\mathbf{RT}_h^1(\Omega) = \left\{ \mathbf{q} \in \mathbf{H}(\text{div}, \Omega) : \mathbf{q}|_T = \mathbf{a}_T + b_T \mathbf{x}, \mathbf{a}_T \in \mathbb{C}^3, b_T \in \mathbb{C}, T \in \mathcal{T}_h \right\}$$

- Basis functions defined on face normals of tetrahedra.
- Constant divergence in each element.
- Completely determined system if their normal components are known on each face.



Remark: Continuity of normal displacements across subdomains can be ensured just by mesh conformality!

Finite Element Method: Matrix Formulation

Writing the variational form in matricial form using \mathbf{RT}_h^1 basis,

$$\int_{\Omega_F} \rho_F c_F^2 \operatorname{div} \mathbf{u} \operatorname{div} \mathbf{v} dV = \mathbf{V}^* \mathbf{K}_F \mathbf{U},$$

$$\int_{\Omega_P} K_P(\omega) \operatorname{div} \mathbf{u} \operatorname{div} \mathbf{v} dV = \mathbf{V}^* \mathbf{K}_P(\omega) \mathbf{U},$$

$$\int_{\Omega_{PML}} \rho_F c_F^2 \tilde{\mathbf{C}}(\nabla \mathbf{u}; \omega) : \nabla \mathbf{v} dV = \mathbf{V}^* \mathbf{K}_{PML}(\omega) \mathbf{U},$$

where, \mathbf{U} and \mathbf{V} contain column vectors whose components are the d.o.f's of \mathbf{u} and \mathbf{v} respectively.

Finite Element Method: Matrix Formulation

Writing the variational form in matricial form using \mathbf{RT}_h^1 basis,

$$\int_{\Omega_F} \rho_F \mathbf{u} \cdot \mathbf{v} \, dV = \mathbf{V}^* \mathbf{M}_F \mathbf{U},$$

$$\int_{\Omega_P} \rho_P(\omega) \mathbf{u} \cdot \mathbf{v} \, dV = \mathbf{V}^* \mathbf{M}_P(\omega) \mathbf{U},$$

$$\int_{\Omega_{PML}} \rho_F \widetilde{\mathbf{M}}(\omega) \mathbf{u} \cdot \mathbf{v} \, dV = \mathbf{V}^* \mathbf{M}_{PML}(\omega) \mathbf{U},$$

where, \mathbf{U} and \mathbf{V} contain column vectors whose components are the d.o.f's of \mathbf{u} and \mathbf{v} respectively.

Finite Element Method: Matrix Formulation

Writing the variational form in matricial form using \mathbf{RT}_h^1 basis,

$$\int_{\Gamma_{\text{MPP}}} (\mathbf{u} \cdot \mathbf{n})(\mathbf{v} \cdot \mathbf{n}) \, dS = \mathbf{V}^* \mathbf{G}_{\text{MPP}} \mathbf{U},$$

$$\int_{\Omega_F} \mathbf{f}_F \cdot \mathbf{v} \, dV = \mathbf{V}^* \mathbf{F}_F,$$

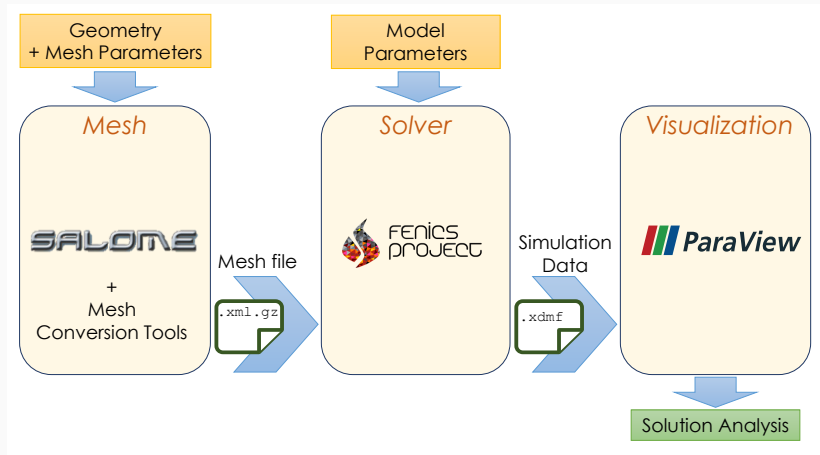
where, \mathbf{U} and \mathbf{V} contain column vectors whose components are the d.o.f's of \mathbf{u} and \mathbf{v} respectively.

Finite Element Method: Matrix Formulation

Writing the variational form in matricial form using \mathbf{RT}_h^1 basis,

$$\left\{ \begin{bmatrix} \mathbf{K}_F & \mathbf{0} & \mathbf{0} \\ \mathbf{0} & \mathbf{K}_P(\omega) & \mathbf{0} \\ \mathbf{0} & \mathbf{0} & \mathbf{K}_{PML}(\omega) \end{bmatrix} + i\omega Z(\omega) \begin{bmatrix} \mathbf{G}_{MPP} & \mathbf{0} & \mathbf{0} \\ \mathbf{0} & \mathbf{0} & \mathbf{0} \\ \mathbf{0} & \mathbf{0} & \mathbf{0} \end{bmatrix} - \omega^2 \begin{bmatrix} \mathbf{M}_F & \mathbf{0} & \mathbf{0} \\ \mathbf{0} & \mathbf{M}_P(\omega) & \mathbf{0} \\ \mathbf{0} & \mathbf{0} & \mathbf{M}_{PML}(\omega) \end{bmatrix} \right\} \begin{bmatrix} \mathbf{U}_F \\ \mathbf{U}_P \\ \mathbf{U}_{PML} \end{bmatrix} = \begin{bmatrix} \mathbf{F}_F \\ \mathbf{0} \\ \mathbf{0} \end{bmatrix}$$
$$\left\{ \mathbf{K} + i\omega Z(\omega) \mathbf{G} - \omega^2 \mathbf{M} \right\} \mathbf{U} = \mathbf{F}$$

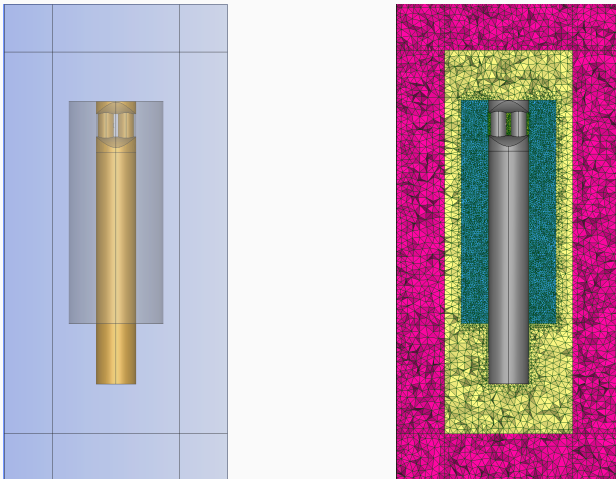
Implementation



Software workflow²

²Bannenberg et al., *Software-based representation of selected benchmark hierarchies equipped with publically available data.*

Geometry and Mesh

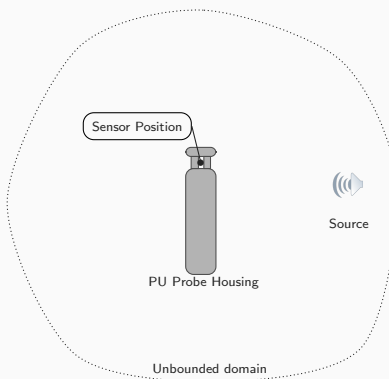


Geometry (*left*) and Mesh (*right*) of the problem setup around the probe is constructed using Salome. Conformal subdomains are highlighted and particularly, probe geometry is overlaid for illustration.

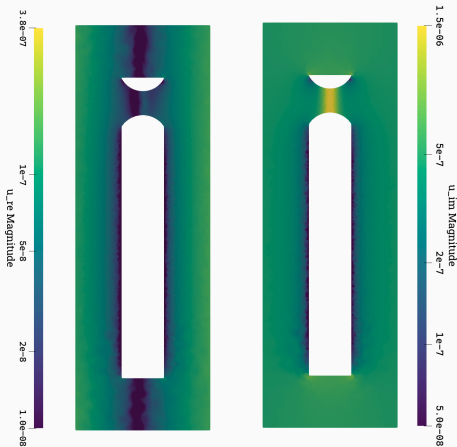
PML Model : Configuration

Simulation configuration for investigating the influence of the probe body,

- Incident plane wave (u_{inc})
- Solve for scattered displacement field,
 $u_{\text{sc}} = u - u_{\text{inc}}$
- Optimal PML absorption function
- Compare with probe design documents

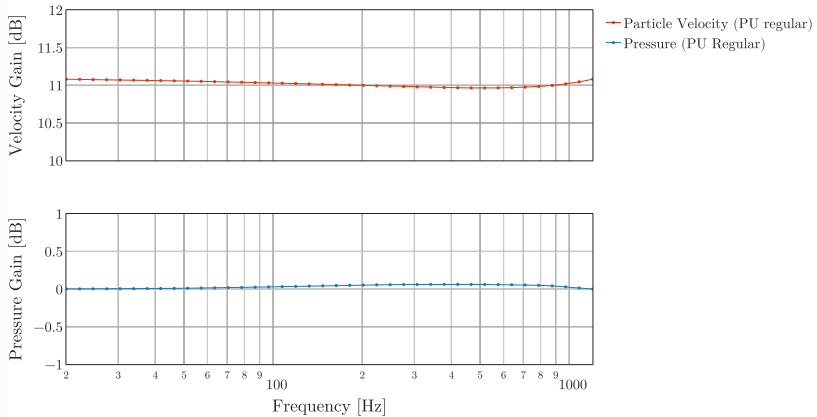


PML Model : Configuration



Contours of total real and imaginary displacement fields for frequency 788.51Hz. The slice is taken amidst the probe pillars with the incident plane wave with the wave number vector parallel to the x-axis.

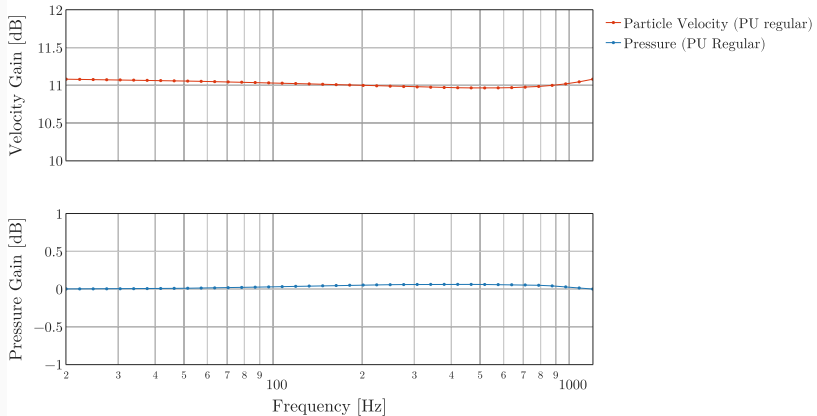
PML Model : Results



$$\text{Velocity gain [dB]} = 20 \log_{10} \left(\frac{\|v_{\text{with}}\|}{\|v_{\text{without}}\|} \right) \text{ with velocity, } v = i\omega u_F(x^*)$$

x^* : Sensor position v_{with} : With housing v_{without} : Without housing

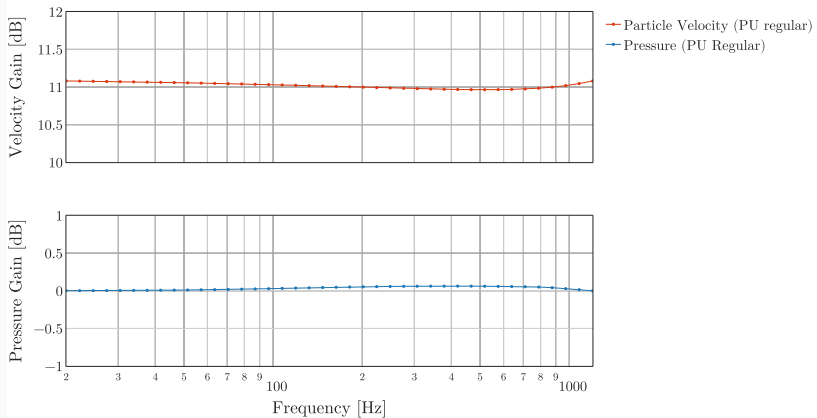
PML Model : Results



Pressure gain [dB] = $20 \log_{10} \left(\frac{|p_{\text{with}}|}{|p_{\text{without}}|} \right)$ with pressure, $p = -\rho_F c_F^2 \operatorname{div} \mathbf{u}_F(\mathbf{x}^*)$

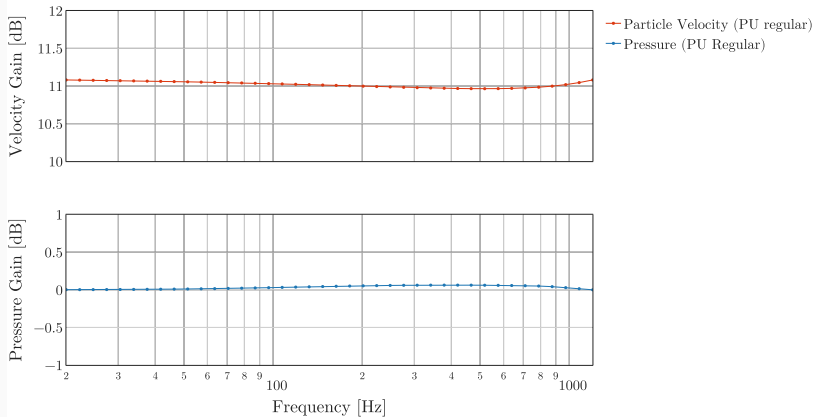
\mathbf{x}^* : Sensor position p_{with} : With housing p_{without} : Without housing

PML Model : Results



Model indicates a 11dB package gain due to the probe housing alone.

PML Model : Results

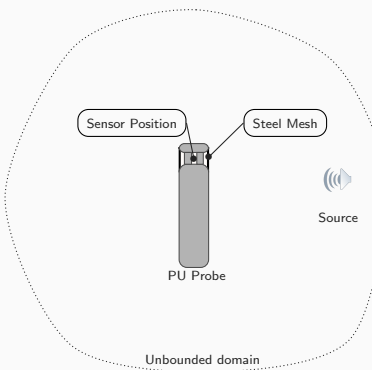


Model indicates a 11dB package gain due to the probe housing alone.
→ Good agreement with design data!

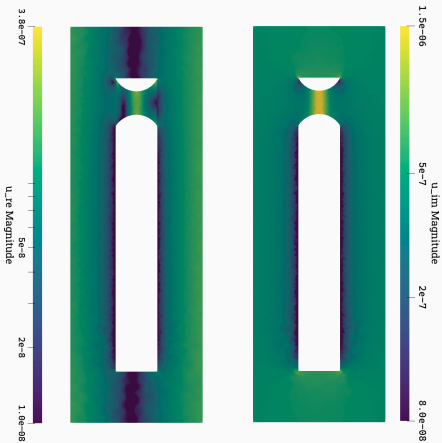
PML + Steel Mesh Model : Configuration

Simulation configuration for investigating the influence of the steel mesh on the probe.

- Incident plane wave (u_{inc})
- Solve for scattered displacement field,
 $u_{\text{sc}} = u - u_{\text{inc}}$
- Optimal PML absorption function
- Steel Mesh parameters obtained from manufacturers
- Compare with preliminary experimental data.

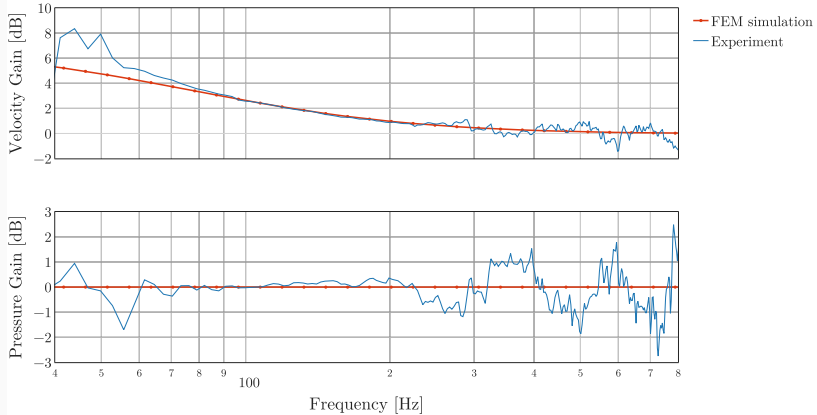


PML + Steel Mesh Model : Configuration



Contours of total real and imaginary displacement fields for frequency 788.51Hz. The slice is taken amidst the probe pillars with the incident plane wave with the wave number vector parallel to the x-axis.

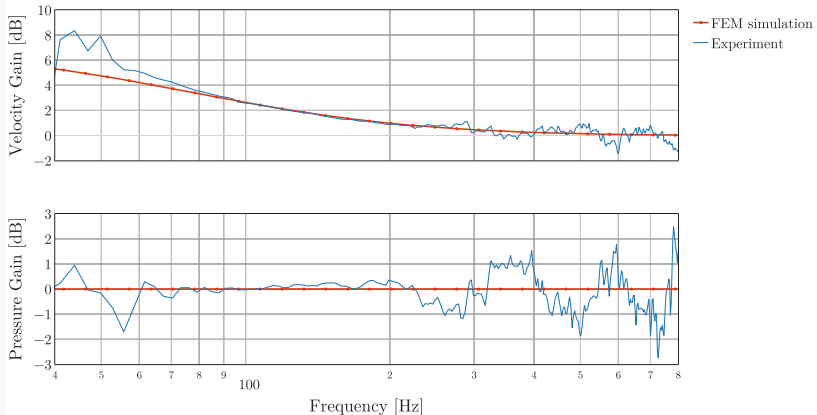
PML + Steel Mesh Model : Results



$$\text{Velocity gain [dB]} = 20 \log_{10} \left(\frac{\|v_{\text{with}}\|}{\|v_{\text{without}}\|} \right) \text{ with velocity, } v = i\omega u_F(x^*)$$

x^* : Sensor position v_{with} : With MPP v_{without} : Without MPP

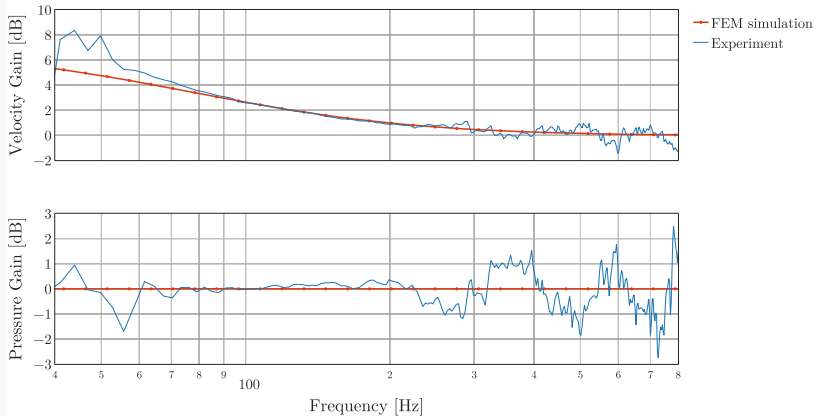
PML + Steel Mesh Model : Results



Pressure gain [dB] = $20 \log_{10} \left(\frac{|p_{\text{with}}|}{|p_{\text{without}}|} \right)$ with pressure, $p = -\rho_F c_F^2 \operatorname{div} \mathbf{u}_F(\mathbf{x}^*)$

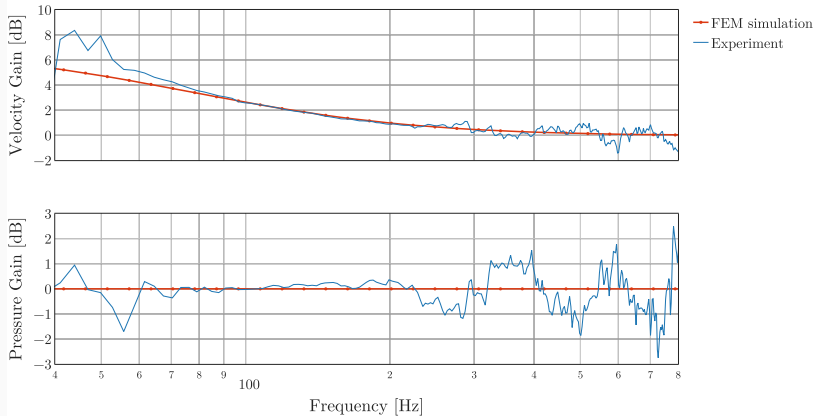
\mathbf{x}^* : Sensor position p_{with} : With MPP p_{without} : Without MPP

PML + Steel Mesh Model : Results



Model shows good agreement with the experimental data!

PML + Steel Mesh Model : Results



Model shows good agreement with the experimental data!
→ More data needed to verify model compliance.

Porous Model parameter fitting: Configuration

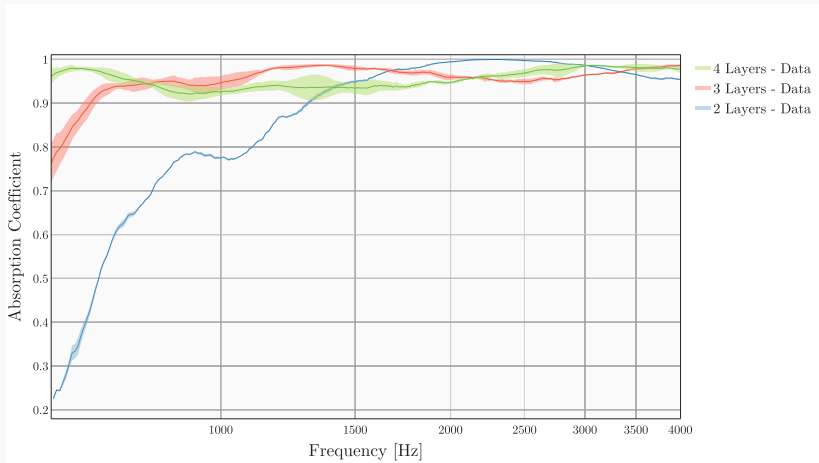


Experimental setup

Measurements performed with

- Fabricated 4 flat melamine layers of equal dimensions
- Rigid wooden backplates
- Anechoic chamber for noise reduction
- Multiple measurements of surface impedance, reflection, absorption for different number of layers

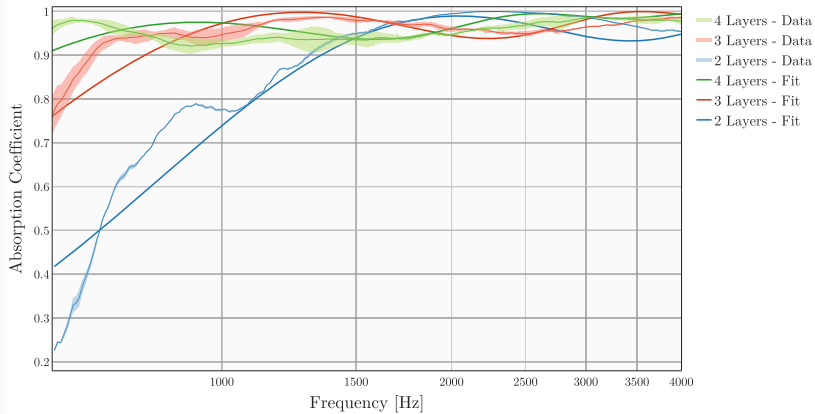
Porous Model parameter fitting: Results



Absorption measurements for different layers of melamine

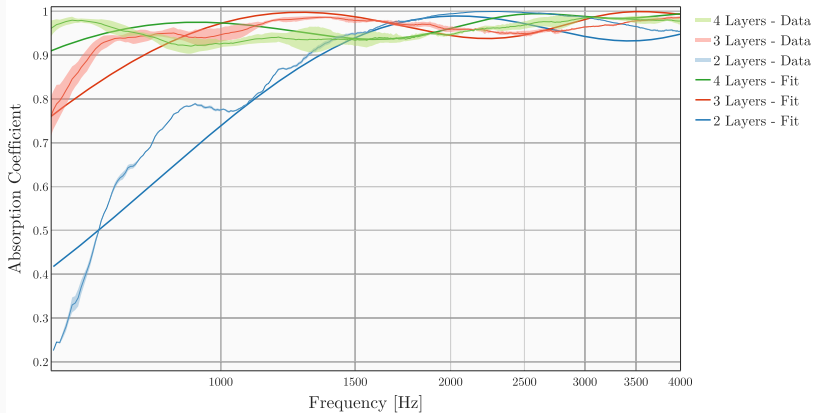
The highlighted regions represent Mean + 2× std.dev of multiple trials.

Porous Model parameter fitting: Results



JCAL parameter fit for measured data

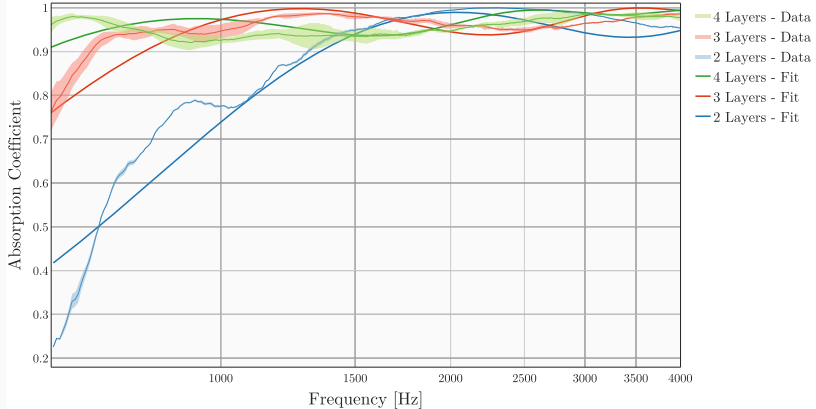
Porous Model parameter fitting: Results



JCAL parameter fit for measured data

- Good fit for higher frequencies,
but not in the lower frequencies favorable for FEM simulations

Porous Model parameter fitting: Results



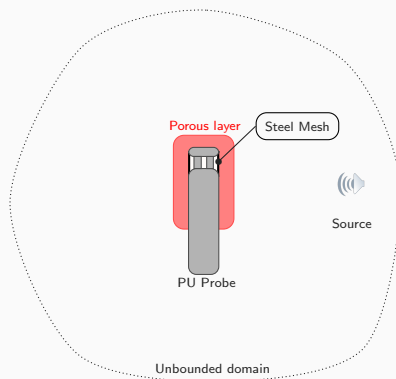
JCAL parameter fit for measured data

→ More data necessary for model compliance!

PML + Steel Mesh + Porous Model : Configuration

Preliminary investigation of the influence of the probe body with steel mesh and a melamine windscreen.

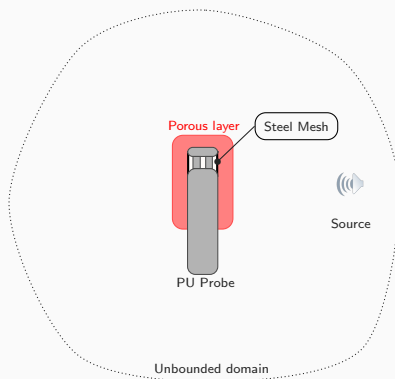
- Incident plane wave (u_{inc})
- Solve for scattered displacement field, $u_{\text{sc}} = u - u_{\text{inc}}$.
- Optimal PML absorption function
- Steel Mesh parameters obtained from manufacturers
- Melamine parameters obtained from inverse method
- Experimental data yet to be obtained



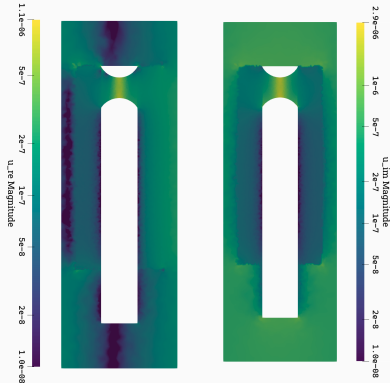
PML + Steel Mesh + Porous Model : Configuration

Preliminary investigation of the influence of the probe body with steel mesh and a melamine windscreens.

- Incident plane wave (u_{inc})
- Solve for scattered displacement field, $u_{\text{sc}} = u - u_{\text{inc}}$.
- Optimal PML absorption function
- Steel Mesh parameters obtained from manufacturers
- Melamine parameters obtained from inverse method
- Experimental data yet to be obtained

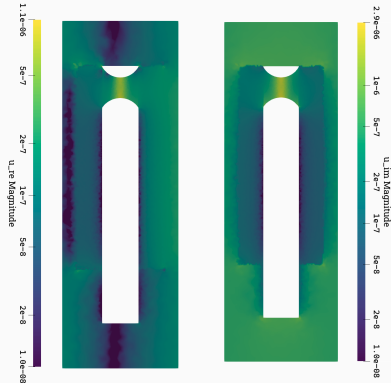


PML + Steel Mesh + Porous Model : Results



Contours of total real and imaginary displacement fields for frequency 800Hz. The slice is taken amidst the probe pillars with the incident plane wave with the wave number vector parallel to the x-axis.

PML + Steel Mesh + Porous Model : Results



Contours of total real and imaginary displacement fields for frequency 800Hz. The slice is taken amidst the probe pillars with the incident plane wave with the wave number vector parallel to the x-axis.

Remark: For lower frequencies ($< 1000\text{Hz}$), the porous model is sensitive to JCAL parameters! *More experimental data and better parametric estimation can help improve the model compatibility.*

Conclusions

- A coupled mathematical model is developed to compute acoustical response accurately using FEM.
- The model is being validated against experimental results and show promising advances.
 - The PML parameter model and steel mesh impedance model in particular.
 - More experimental data necessary to ascertain reliability and applicability of the models for acoustic measurements.
 - For further model development, flow models are being investigated.

References i

-  Allard, J. and N. Atalla. *Propagation of Sound in Porous Media: Modelling Sound Absorbing Materials* 2e. Wiley, 2009. ISBN: 9780470747346. DOI: 10.1002/9780470747339.
-  Bannenberg, Marcus et al. *Software-based representation of selected benchmark hierarchies equipped with publically available data*. Version 2.0. Project Deliverable (D5.2), Version 2.0. June 2020. DOI: 10.5281/zenodo.3888145. URL: <https://doi.org/10.5281/zenodo.3888145>.
-  Bermúdez, A. et al. "An optimal perfectly matched layer with unbounded absorbing function for time-harmonic acoustic scattering problems". In: *Journal of Computational Physics* 223.2 (2007), pp. 469–488. ISSN: 0021-9991. DOI: 10.1016/j.jcp.2006.09.018.
-  Champoux, Yvan and Jean-F Allard. "Dynamic tortuosity and bulk modulus in air-saturated porous media". In: *Journal of Applied Physics* 70.4 (1991), pp. 1975–1979.

References ii

-  Maa, Dah-You. "Microperforated-Panel Wideband Absorbers". In: *Noise Control Engineering Journal* 29.3 (Nov. 1, 1987), pp. 77–84. ISSN: 0736-2501. DOI: 10.3397/1.2827694.
-  Río Martín, Laura del. "Numerical characterization of complex materials and vibro-acoustic systems". PhD thesis. University of ACoruña, 2020.
-  Sagartzazu, X, L Hervella-Nieto, and JM Pagalday. "Review in sound absorbing materials". In: *Archives of Computational Methods in Engineering* 15.3 (2008), pp. 311–342.
-  Tijs, Emiel. "Study and development of an in situ acoustic absorption measurement method". ISBN: 9789036535212. PhD thesis. Enschede, The Netherlands: University of Twente, 2013. DOI: 10.3990/1.9789036535212.